Journal of Materials Chemistry B

Accepted Manuscript

ROYAL SOCIETY OF CHEMISTRY

www.rsc.org/materialsB

Journal Name

RSCPublishing

ARTICLE

A facile approach to biodegradable polydisulfide MRI contrast agent

Cite this: DOI: 10.1039/x0xx00000x

Weiren Cheng,[a,c] Reshmi Rajendran,[b] Wei Ren,[a] Liuqun Gu,[a] Yong Zhang,[c] Kai-Hsiang Chuang[b] and Ye Liu[a*]

Received 00th January 2012,
Accepted 00th January 2012

DOI: 10.1039/x0xx00000x

www.rsc.org/

Polydisulfide MRI contrast agent was obtained by grafting diethylenetriaminepentaacetic (DTPA) to disulfide-containing poly(amido amine)s-graft-poly(ethylene glycol) (PEG) followed by forming Gd(III) chelates. Self-assemble of the MRI contrast agent obtained occurs in aqueous solution forming nanosized micelles with PEG shells and ionic complex cores. The chemistry and structures of the MRI contrast agent and assembly were characterized using NMR, GPC and DLS. Thiol-induced degradation of the backbone and the assembly of the MRI contrast agent were investigated using GPC and DLS, respectively, and a readily degradation was observed. Poly(BAC-AMPD)-*g*-PEG-*g*-Gd-DTPA also shows a low cytotoxicity and a high r_1 value, so it is promising to provide better MRI imaging with lower side effects.

Introduction

Magnetic resonance imaging (MRI) is a powerful, non-invasive and non-radioactive diagnostic imaging technique which can provide high spatial resolution and multiple physical and physiological contrasts. MRI contrast agents are typically needed to improve the quality of imaging for more accurate diagnosis of diseases.[1,2] Currently, MRI contrast agents used in clinic are small molecular gadolinium (III) (Gd(III)) chelates such as Magnevist®, Eovist® and Dotarem®. However, these MRI contrast agents have their limitations including short retention time and fast vascular extravasation due to their low molecular weight.[3] One of the approaches to overcome these limitations is to integrate Gd(III) chelates with polymers to form macromolecular MRI contrast agents which display slow vascular extravasation,[1,4-8] together with capability to target tumor and higher T_1 relaxivity.[1,4-7,9,10] However, the slow and incomplete elimination of Gd(III) ions integrated in these macromolecules can result in side effects such as nephrogenic systemic fibrosis (NSF) especially in renal dysfunctional patients.[11-13] Therefore, macromolecular MRI contrast agents with suitable degradation profile are needed for feasible excretion of Gd(III) chelates after imaging.[14]

Several types of biodegradable polydisulfide Gd(III) based macromolecular MRI contrast agents were reported with Gd(III) chelates being either linked together or conjugated to polymer via disulfide bonds.[14-18] Linear macromolecular Gd(III) based MRI contrast agents with disulfide in the backbone were prepared by copolymerization of diethylenetriaminepentaacetic (DTPA) dianhydride and disulfide containing diamine, followed by forming Gd(III) complexation to produce Gd-DTPA diamide which has low chelating stability.[14] These linear macromolecular Gd(III) based MRI contrast agents showed a prolonged retention time together with an improved *in vivo* contrast, are degradable, and are readily excreted via renal filtration.[15-17] Recently a new type of polydisulfide Gd(III) based contrast agent with a higher chelating stability was prepared by condensation polymerization of a special diamine monomer with chelate units and disulfide containing activated dianhydride followed by forming Gd(III) chelates.[18]

Here we report a facile approach to biodegradable polydisulfide MRI contrast agent. As shown in Scheme 1, the disulfide-containing poly(amido amine)s, poly(BAC-AMPD), was synthesized via Michael addition polymerization of trifunctional amine, 4-(aminomethyl)piperidine (AMPD), and an equimolar of diacrylamide, *N,N*-cystaminebis(acrylamide) (BAC). Then poly(ethylene glycol) (PEG) and DTPA were conjugated via the reactions with the secondary amine, respectively, to form poly(BAC-AMPD)-*g*-PEG-*g*-DTPA. Macromolecular MRI contrast agent, poly(BAC-AMPD)-*g*-PEG-*g*-Gd-DTPA, was obtained by forming chelates with Gd(III) ion. The self-assembly behaviour, thiol-induced degradation, *in vitro* cytotoxicity and the relaxivity of poly(BAC-AMPD)-*g*-PEG-*g*-Gd-DTPA were investigated.

Scheme 1.

Experimental Section

Materials

BAC was from Polysciences, Inc, AMPD (99%) was from Alfa Aesar, and DTPA dianhydride (98%), gadolinium (III) chloride hexahydrate, L-dithiothreitol (DTT), L-glutathione reduced (GSH) and xylenol orange sodium salt indicator were from Sigma Aldrich. Monomethyl PEG (~2000 g/mol) 4-nitrophenyl carbonate was prepared using the method reported.[19] The other chemicals of reagent grade were used as received.

MCF-7 (human breast adenocarcinoma) cells and HepG2 (human hepatoma) cells were obtained from American Type Culture Collection (ATCC, Rockville, MD). They were maintained in Dulbecco's modified eagle medium (DMEM, invitrogen) with 10% fetal bovine serum (FBS), 2 mM glutamine, 100 units/ml penicillin and 100 μg/ml streptomycin at 37 °C in an incubator with 5% CO_2 atmosphere.

Synthesis of poly(BAC-AMPD)

3.08 g (26.7 mmol) of AMPD were added into 40 mL of anhydrous methanol containing 6.96 g (26.7 mmol) of BAC under stirring and argon purging at room temperature. After 1 month, 0.03 g (0.27 mmol) of AMPD was added, and the reaction was performed for 1 more day. Then the solution was dialyzed in methanol using membrane with a molecular weight cutting off of 2000.

Preparation of poly(BAC-AMPD)-*g*-PEG-*g*-DTPA

10.17 g (4.5 mmol) of monomethyl PEG 4-nitrophenyl carbonate was added into 6.78 g (18 mmol) of dried poly(BAC-AMPD) in 85 mL of anhydrous dimethyl sulfoxide (DMSO) under stirring and argon purging at room temperature. 5 days later, the solution was dialyzed in methanol using membrane with a molecular weight cutting off of 3500.

0.50 g (0.63 mmol) of dried poly(BAC-AMPD)-*g*-PEG in 6 mL of anhydrous DMSO was added dropwise into 9 mL of anhydrous DMSO containing 0.89 g (2.5 mmol) of DTPA dianhydride and 0.385 mL (2.7 mmol) of TEA at 50 °C under stirring and argon purging. 24 hours later, the solution was dialyzed in deionized (DI) water using membrane with a molecular weight cutting off of 1000 MWCO followed by lyophilized drying.

Complexation of poly(BAC-AMPD)-*g*-PEG-*g*-DTPA with Gd(III)

0.04 g (0.11 mmol) of gadolinium (III) chloride hexahydrate was added into 5 mL of deionized water containing 0.12 g of poly(BAC-AMPD)-*g*-PEG-*g*-DTPA at pH 5.5 under stirring at room temperature for overnight. Then excess gadolinium (III) chloride hexahydrate was removed by dialysis in deionized water using membrane with a molecular weight cutting off of 1000. Xylenol orange sodium salt indicator was used to ensure a complete removal of Gd(III) ions. After all the Gd(III) ions were removed, the solution was lyophilized. Poly(BAC-AMPD)-*g*-PEG-*g*-Gd-DTPA was dissolved in deionized water for characterization.

***in vitro* cytotoxicity of poly(BAC-AMPD)-*g*-PEG-*g*-Gd-DTPA**

Cytotoxicity of poly(BAC-AMPD)-*g*-PEG-*g*-Gd-DTPA was evaluated in MCF-7 and HepG2 cell lines. Viability of the cells was assessed by the standard thiazolyl blue [3-(4,5-dimethyliazolyl-2)-2,5-diphenyl tetrazolium bromide] (MTT) assay. This colorimetric assay allows determination of the number of viable cells through the metabolic activity of the cells.

The cancer cells were seeded in 96-well plates with a seeding density of 10,000 cells/well and were cultured in DMEM supplemented with 10% FBS and 1% penicillin-streptomycin solution in an incubator at 37°C, 5% CO_2, and 95% relative humidity. The cells were allowed to adhere to the well bottom upon overnight incubation. Then the medium was replaced with the sample solutions of different concentrations. Meanwhile, wells containing only cell culture medium were prepared as untreated controls. At the predetermined time, the medium containing samples was aspirated and the wells were washed with 1 ×PBS solution for two times to removed non-internalized sample. Then 100 μL of DMEM and 10 μL of MTT solution (5 mg/mL in 1 ×PBS solution) were added to the wells. After incubation for 4 h at 37 °C, the solution was removed and the formazan precipitate was dissolved in 100 μL of dimethylsulfoxide (DMSO). The absorbance intensity of the solution was then quantified spectrophotometrically using a microplate reader (TECAN SpectraFluor Plus) at 570 nm. Cell viability was expressed by the following equation:

$$\text{Cell viability (\%)} = \text{Abs}_{\text{sample}} / \text{Abs}_{\text{control}} \times 100\%$$

Where $\text{Abs}_{\text{sample}}$ was the absorbance for cells treated with samples, while $\text{Abs}_{\text{control}}$ was the absorbance for untreated control cells. All the tests were performed in multiples.

Degradation studies of poly(BAC-AMPD) and micelles of poly(BAC-AMPD)-*g*-PEG-*g*-Gd-DTPA

5.0 mg/mL of poly(BAC-AMPD) in pH 4.5 acetate buffer solution was treated with 10 mM of DTT at 37 °C under stirring for 2 h. GPC was applied to monitor the change in the molecular weight profile.

0.5 mg/mL of poly(BAC-AMPD)-*g*-PEG-*g*-Gd-DTPA in DI water was treated with 20 μM of GSH at 37 °C under stirring for certain time. Small amount of the samples were taken for dynamic light scattering measurement.

MRI T_1relaxivity measurement

A multi-slice localization scan was used to acquire images in the transverse section (i.e. the transverse section of the barrel of the syringe) along the length of the syringes containing the sample. The multi-slice images acquired were assessed to select slices with minimal heterogeneity and absence of bubbles. T_1 mapping was carried out using an inversion recovery spin-echo sequence with inversion times (Tis): 31, 50, 100, 200, 400, 600, 800, 1000, 1500, 2000, 3500 and 9980 ms with FOV = 56 × 75 mm, TE = 6.9 ms, TR = 10000 ms, slice thickness of 2 mm and

number of slices = 1. The data was analysed using Matlab and the T_1 relaxivity calculated from homogenous regions within each sample using AMIDE as shown in Figure 7. Relaxivity, the slope of relaxation rates as a function of the concentrations of the contrast agent, was then calculated.

Measurements

The molecular weight and molecular weight distribution of poly(BAC-AMPD) was measured on a Waters 2690 apparatus with two columns in series (Waters Ultrahydrogel 250 and 200) and a Waters 410 refractive index detector. The eluent was pH 4.5 acetate buffer solution with a flow rate of 0.6 mL/min, and poly(ethylene oxide) standards were used. ^{13}C and ^{1}H nuclear magnetic resonance (NMR) characterization were performed on Bruker 400 MHz NMR spectrometer with methanol-d_4 and deuterium oxide (D_2O) as solvent. The number of Gd(III) chelated was measured using the Dual-view Optima 5300 DV inductively coupled plasma optical emission spectrometry (ICP-OES). The hydrodynamic size and critical micelle concentration (CMC) of micelles prepared were determined using Brookhaven dynamic lightering scattering (DLS) instrument at 90^o (632.8 nm) using NNLS analysis. The micelles were also viewed under a high resolution Philips CM300 transmission electron microscope (FEGTEM). The MRI experiments were carried out on a 7T MRI (ClinScan, Bruker Biospin GmbH, Germany) with a 20 cm bore size and a high performance gradient and shim coil (gradient strength of 63 G/cm, slew rate of 6300 T/m/s) interfaced to a Siemens console. A volume coil (diameter: 72 mm) was used for RF transmit and receive. The samples were placed at the isocentre of the magnet/coil.

Results and Discussion

Synthesis of poly(BAC-AMPD)-*g*-PEG-*g*-Gd-DTPA

As shown in Scheme 1, poly(BAC-AMPD) was synthesized via Michael addition polymerization of AMPD and an equimolar BAC in methanol. Although the reactivity sequence of the amines in AMPD were 2^o amine (original) > 1^o amine >> 2^o amine (formed),[20,21] the 2^o amine (formed) participated in the polymerization process, which resulted in formation of poly(BAC-AMPD) with ~20% branching units determined from ^{13}C NMR spectrum.[22] In comparison with the mixture solvent of water and DMSO, the polymerization in methanol can provide poly(BAC-AMPD) with a higher molecular weight and ~20% branching.[22] Because a higher molecular weight is preferred for preparation of macromolecular MRI contrast agent, and the effect of branching might not be significant,[14-18] here poly(BAC-AMPD) is prepared using methanol as solvent. Poly(BAC-AMPD) obtained is soluble in methanol and DMSO, but insoluble in water. Figure 1a and 2a show GPC profile in pH 4.5 acetate buffer solution and ^{1}H NMR spectrum of poly(BAC-AMPD) obtained in methanol-d_4, respectively. The molecular weight distribution of poly(BAC-AMPD) is wide with a polydispersity index (PDI) of 2.6 which is reasonable for polymers obtained from multistage polymerization.[20] The two peaks in the GPC curve correspond to M_p of ca. 14034 and 1000 g/mol, respectively.

Figures 1 and 2.

PEG was grafted to poly(BAC-AMPD) via forming urethane groups through the reaction with the secondary amines in the backbone of poly(BAC-AMPD).The feed molar ratio of PEG to the 2^o amine in poly(BAC-AMPD) was kept at 1.25 : 5 to control the amount of PEG grafted in order to retain some of the secondary amines for further functionalization. The molar ratio of the grafted PEG and BAC-AMPD unit was determined to be 1: 5 using equation 1:

$$\text{Molar ratio of PEG/BAC-AMPD} = I_{4.20} / I_{1.29} \quad (1)$$

Where $I_{4.20}$ and $I_{1.29}$ are the integral intensities of the peaks at 4.20 ppm and 1.29 ppm in Figure 2b, respectively.

Figures 2b and 2c shows ^{1}H NMR spectra of poly(BAC-AMPD)-*g*-PEG in methanol-d_4 and D_2O, respectively. In comparison with Figure 2b, the peaks attributed to poly(BAC-AMPD) can still be observed but are noticeably broader in Figure 2c. The relative peak intensity of the peaks in ^{1}H NMR spectrum is related to the mobility of the protons, and a broad and less intensive peak of a proton is caused by lower mobility in the solution.[22-25] Therefore the mobility of poly(BAC-AMPD) in poly(BAC-AMPD)-*g*-PEG in aqueous solution is not as good as in methanol, however, no species with a diameter higher than 10 nm could be observed in aqueous solution formed by directly dissolving poly(BAC-AMPD)-*g*-PEG in water using DLS.

DTPA was conjugated to poly(BAC-AMPD)-*g*-PEG via the reaction with the remaining secondary amines in poly(BAC-AMPD) to form amide bonds as illustrated in Scheme 1. Figure 2d shows the ^{1}H NMR spectrum of poly(BAC-AMPD)-*g*-PEG-*g*-DTPA in D_2O at pH 5.5. The grafting of DTPA is confirmed by the appearance of the characteristic peaks such as the peaks at 3.7 ppm.[23,26] However, the content of conjugated DTPA cannot be determined using ^{1}H NMR due to the self-assembly discussed below.

Poly(BAC-AMPD)-*g*-PEG-*g*-Gd-DTPA was obtained through forming Gd(III) chelates. The content of Gd(III) ions was determined using ICP-OES, and the result indicates that 1.9 out of 5 units of BAC-AMPD were complexed with Gd(III) ions. The composition of poly(BAC-AMPD)-*g*-PEG-*g*-Gd-DTPA is summarized in Table 1.

Table 1.

Self-assembly of poly(BAC-AMPD)-*g*-PEG-*g*-Gd-DTPA in aqueous solution

Self-assembly of poly(BAC-AMPD)-*g*-PEG-*g*-Gd-DTPA occurred in aqueous solution. Figure 3 shows TEM images of

the micelles formed from the self-assembly of poly(BAC-AMPD)-*g*-PEG-*g*-Gd-DTPA with or without osmium(VIII) oxide staining. Dark irregular regions can be observed in the micelles without osmium(VIII) oxide staining as shown in Figure 3a. These dark regions were confirmed to be rich in Gd(III) ions through energy dispersive X-ray spectroscopy. This indicates that Gd(III) are chelated with polymer and the conjugated Gd(III) chelates are integrated in the self-assembly of poly(BAC-AMPD)-*g*-PEG-*g*-Gd-DTPA. After staining with osmium(VIII) oxide as shown in Figure 3b, larger dark areas are observed, and the diameter of the micelles was ca. 113 nm in dry state. The hydrodynamic size of the micelles in aqueous solution was determined to be ca. 188 nm using DLS. The critical micelle concentration (CMC) of poly(BAC-AMPD)-*g*-PEG-*g*-Gd-DTPA in aqueous solution was determined to be ca. 60.2 μg/mL by plotting the average scattering intensity against the polymer concentrations as illustrated in Figure 4.[22,28]

Figures 3 and 4.

The structure of the self-assembly of poly(BAC-AMPD)-*g*-PEG-*g*-Gd-DTPA could not be investigated using ^{1}H NMR due to the existence of Gd(III). However, the self-assembly profile of the precursor of poly(BAC-AMPD)-*g*-PEG-*g*-DTPA could be investigated using ^{1}H NMR. As shown in Figure 2d, the integral intensities of the peaks of protons adjacent to amines unit, i.e., peaks m and n, are reduced in comparison with those peaks t and s in the middle part of BAC. Meanwhile, the peaks of PEG are still obvious. This reflects that the self-assembly leads to a restricted mobility of these segments containing amines. Therefore, the self-assembly should be due to the formation of the ionic complex between the cationic amines of AMPD and the anionic carbonate groups of DTPA. The ionization degree of the amine and carboxylic acid depends on pH; and a perfect polyelectrolyte complex is formed between cationic polymer and anionic polymer with an equimolar ratio of cationic and anionic group together with the same polymer length.[29] Here there are different types of amines and carboxylic acid which have different pKa value,[27,30] therefore different ionization profiles of the amine and carboxylic acid exist and result in a complicated pH dependence of the ionic complex. This is demonstrated by a relative lower integral intensity of the peak d attributed to DTPA related to the peak s attributed to BAC in ^{1}H NMR spectrum of the assembly at pH 7 (Figure 2e) in comparison with at pH 5 (Figure 2d). After Gd(III) ions was introduced, the formation of ionic complex with Gd(III) ions involved is still possible, and the self-assembly of poly(BAC-AMPD)-*g*-PEG-*g*-Gd-DTPA should be composed of the ionic complex cores and PEG shells.

The cytotoxicity of poly(BAC-AMPD)-*g*-PEG-*g*-Gd-DTPA was evaluated in MCF-7 and HepG2 cell lines. A low cytotoxicity was observed. Ca. 80% and 90% of MCF-7 and HepG2 cells were still viable after incubation with 200 μM of the polymer for 24 h, respectively, as shown in Figure 5.

Figure 5.

Degradation of poly(BAC-AMPD)-*g*-PEG-*g*-Gd-DTPA

Thiol-induced degradation of the backbone of poly(BAC-AMPD)-*g*-PEG-*g*-Gd-DTPA occurs readily. As shown in Figure 1b, almost complete degradation of poly(BAC-AMPD) can be observed in pH 4.5 acetate buffer solution in the presence of 10 mM of DTT after 2 h at 37 ^{o}C. Due to the formation of micelles, thiol-induced degradation of poly(BAC-AMPD)-*g*-PEG-*g*-Gd-DTPA could not be monitored using GPC. Instead the degradation of the micelles of poly(BAC-AMPD)-*g*-PEG-*g*-Gd-DTPA was monitored using DLS. Figure 6 shows the change in the DLS profile of the micelles from 0.5 mg/mL of poly(BAC-AMPD)-*g*-PEG-*g*-Gd-DTPA in DI water at 37^{o}C in the presence of 20 μM of GSH which is close to the concentration of GSH in biological extracellular matrix. The scattering intensity decreases by 15% in 15 minutes of incubation, and another 10% and 40% in 60 minutes and 2 hours, respectively. At this stage, no obvious change in the diameter of the micelles is observed. However, an increase in the diameter of the micelles becomes significant from ca. 206 nm at 2 h to ca. 512 nm at 24 h.

The micelles are composed of the ionic complex cores and PEG shells, and GSH diffuses into the PEG shells more easily than into the ionic complex cores; hence the PEG segments are removed first. When a part of the PEG shells is removed without leading to formation of aggregate, the light scattering intensity proportional to the mass of the assembly decreases. After more PEG shells are removed leading to formation of aggregate, the size of the assembly increases. Due to a low concentration of GSH used, no significant change in scattering intensity and size can be observed in 2 h of incubation, which is similar to the degradation profile of the nanosized complex of disulfide-containing poly(amido amine)s and DNA in the presence of 10 μM of DTT.[31] Here the molar ratio of GSH / disulfide bond is only 1 / 25 when a plasma GSH concentration of 20 μM was adopted, however, an obvious degradation of the assembly of poly(BAC-AMPD)-*g*-PEG-*g*-Gd-DTPA could be observed already, and a feasible degradation *in vivo* can be expected with ample thiol compound being presented.

Figure 6.

Relaxivity of poly(BAC-AMPD)-*g*-PEG-*g*-Gd-DTPA

To determine the relaxivity (r_1) of the micelles of poly(BAC-AMPD)-*g*-PEG-*g*-Gd-DTPA, the longitudinal relaxation time (T_1) of different Gd(III) concentrations were measured and the results are listed in Figure 7. The micelles exhibited a r_1 value of 5.90 ± 0.09 $mM^{-1}s^{-1}$ which is 50% higher than Gd-DTPA (~ 4 $mM^{-1}s^{-1}$)[32,33]. The micelles have higher r_1 than most small molecular Gd(III) based contrast agents, due to the reduced molecular tumbling.[2,34]

Figure 7.

The self-assembly of poly(BAC-AMPD)-*g*-PEG-*g*-Gd-DTPA probably can provide a longer MRI imaging window because of a longer retention time due to reduced vascular extravasation, and an enhanced signal of T_1-weighted MRI mapping because of a passive targeted accumulation due to the enhanced permeation and retention (EPR) effects[35] in comparison with small molecular MRI contrast agent, i.e., Gd-DTPA, after administration in vivo. After imaging function, poly(BAC-AMPD)-*g*-PEG-*g*-Gd-DTPA can be degraded to species smaller than the renal clearance threshold via reaction with thiol compounds presented in extracellular matrix, i.e., GSH, cysteine, homocysteine and cysteinylglycine,[36] and the degradation products can excreted feasibly via renal filtration resulting in no accumulation of Gd(III) ions in the body, as other types of polydisulfide macromolecular MRI contrast agents reported.[15-17]

Conclusions

DTPA were conjugated to poly(BAC-AMPD)-*g*-PEG via the reaction with 2^o amines of poly(BAC-AMPD). The obtained MRI contrast agent has a payload of Gd(III) chelates to be 20% of BAC-AMPD units. Micelles can be formed from Poly(BAC-AMPD)-*g*-PEG-*g*-Gd-DTPA in aqueous solution with the PEG shells and the ionic complex cores from the cationic amines and anionic carbonate groups. With a low cytotoxicity, a readily thiol-induced degradation and a higher r_1, poly(BAC-AMPD)-*g*-PEG-*g*-Gd-DTPA is promising for producing better MRI imaging with lower side effects.

Acknowledgements

The financial support is from A*Star under JCO programme, JCO DP programme, Biomass programme and Personal Care programme.

Notes

[a] Institute of Materials Research and Engineering, A*STAR (Agency for Science, Technology and Research), 3 Research Link, 117602, Singapore. E-mail: ye-liu@imre.a-star.edu.sg
[b] Singapore Bioimaging Consortium, A*STAR (Agency for Science, Technology and Research), 11 Biopolis Way, #01-02 Helios Building, 138667, Singapore.
[c] Department of Bioengineering, National University of Singapore, 9 Engineering Drive 1, Block EA #03-12, 117575, Singapore.

References

1 P. Caravan, J. J. Ellison, T. J. McMurry, R. B. Lauffer, *Chem. Rev.*, 1999, **99**, 2293-2352.
2 W. Cheng, Y. Ping, Y. Zhang, K. H. Chuang, Y. Liu, *J. Healthcare Eng.*, 2013, **4**, 23-46.
3 A. Bumb, M. W. Brechbiel, P. Choyke, *Acta Radiol.*, 2010, **51**, 751-767.
4 S. Mornet, S. Vasseur,F. Grasset, E. J. Duguet, *Mater. Chem.*, 2004, **14**, 2161-2175.
5 S. E. Matthews, C. W. Pouton, M. D. Threadgill, *Ad., Drug Deliv. Rev.*, 1996, **18**, 219-267.
6 A. Accardo, D. Tesauro, L. Aloj, C. Pedone, G. Morelli, *Coord. Chem. Rev.*, 2009, **253**, 2193-2213.
7 S. Langereis, A. Dirksen, T. M. Hackeng, M. H. P. Van Genderen, E. W. Meijer, *New J. Chem.*, 2007, **31**, 1152-1160.
8 L. Villaraza, A. Bumb, M. W. Brechbiel, *Chem. Rev.*, 2010, **110**, 2921-2959.
9 R. Brasch, C. Pham, D. Shames, T. Roberts, K. Van Dijke, N. Van Bruggen, J. Mann, S. Ostrowitzki, O. J. Melnyk, *Magn. Reson. Im.*, 1997, **7**, 68-74.
10 Z. R. Lu, F. Ye, A. Vaidya, *J. Control. Release*, 2007, **122**, 269-277.
11 A. Deo, M. Fogel, S. E. Cowper, *Clin. J. Am. Soc. Nephrol.*, 2007, **2**, 264-267.
12 P. H. Kuo, E. Kanal, A. K. Abu-Alfa, S. E. Cowper, *Radiology*, 2007, **242**, 647-267.
13 H. S. Thomsen, P. Marckmann, V. B. Logager, *Cancer Imaging*, 2007, **7**, 130-137.
14 Z. R. Lu, A. M. Mohs, Y. Zong, Y. Feng Y, *Int. J. Nanomedicine*, 2006, **1**, 31-40.
15 Y. Zong, X. Wang, K. C. Goodrich, A. M. Mohs, D. L. Parker, Z. R. Lu, *Magn. Reson. Med.*, 2005, **53**, 835-842.
16 Y. Zong, X. Wang, E. K. Jeong, D. L. Parker, Z. R. Lu, *Mag. Reson. Imaging*, 2009, **27,** 503-511.
17 Y. Zong, J. Guo, T. Ke, A. M. Mohs, D. L. Parker, Z. R. Lu, *J. Control. Release*, 2006, **112**, 350-356.
18 Z. Ye, X. Wu, M. Tan, J. Jesberger, M. Grisworld, Z. R. Lu, *Contrast Media Mol. Imaging*, 2013, **8**, 220-228.
19 C. L. Lay, H. Q. Liu, D. Wu, Y. Liu, *Chem. Eur. J.*, 2010, **16**, 3001-3004.
20 D. Wu, Y. Liu, C. He, T. Chung, S. Goh, *Macromolecules*, 2004, **37**, 6763-6770.
21 D. Wang, Y. Liu, Z. Hu, C. Hong, C. Pan, *Polymer*, 2005, **46**, 3507-3514.
22 W. Cheng, J. N. Kumar, Y. Zhang, Y. Liu, *Macromol. Biosci.* 2014, 14, 347.
23 J. V. M. Weaver, Y. Q. Tang, S. Y. Liu, P. D. Iddon, R. Grigg, N. C. Billingham, S. P. Armes, R. Hunter, S. P. Rannard, *Angew. Chem., Int. Ed.*, 2004, **43**, 1389-1392.
24 Y. Li, B. S. Lokitz, C. L. McCormick, *Angew. Chem., Int. Ed.*, 2006, **45**, 5792-5795.
25 C. L. Lay, H. R. Tan, X. H. Lu, Y. Liu, *Chem. Eur. J.*, 2011, **17**, 2504-2509.
26 E. Nakamura, K. Makino, T. Okano, T. Yamamoto, M. Yokoyama, *J. Control. Release*, 2006, **114**, 325-333.
27 K. A. Deal, R. J. Motekaitis, A. E. Martell, M. J. Welch,*J. Med. Chem.*, 1996,**39**, 3096-3106.
28 H. Hussain,B. H. Tan, C. S. Gudipati, C. B. He, Y. Liu, T. P. Davis, *Langmuir*, 2009, **25**, 5557-5564.
29 A. Harada, K. Kataoka, *Science, 1999,* **283**, 65-67.
30 G. B. Sun, D. Wu, Y. Liu, C. B. He, T. S. Chung, S. H. Goh, *Polymer*, 2005, **46**, 3355-3362.
31 Y. Ping, D C Wu, J. N. Kumar, W. R. Cheng, C. L. Lay, Y. Liu, *Biomacromolecules*, 2013, **14**, 2083-2094.
32 J. Bremerich, D. Bilecen, P. Reimer, *Eur. Radiol.*, 2007, **17**, 3017-3024.

33 W. L. Zhang, D. W. Yong, J. Huang, J. H. Yu, S. Y. Liu, M. X. Fan, *J. Applied Polym. Sci.*, 2011, **120**, 2596-2605.
34 L. Yang, B. Mariana, L. Sophie, E. Luce vande, N. M. Robert, T. T. D. Hien, *Macromolecules*, 2012, **45**, 4196-4204.
35 H. Maeda, H. Nakamura, J. Fang. *Ad., Drug Deliv. Rev.*, *2013,* **65,** 71-79.
36 A. Anderson, A. Lindgren, B. Hultberg. *Clin. Chem.*, 1995, **41**, 361-366.

FIGURES AND SCHEMES

Scheme 1. Synthesis of poly(BAC-AMPD)-*g*-PEG-*g*-Gd-DTPA.

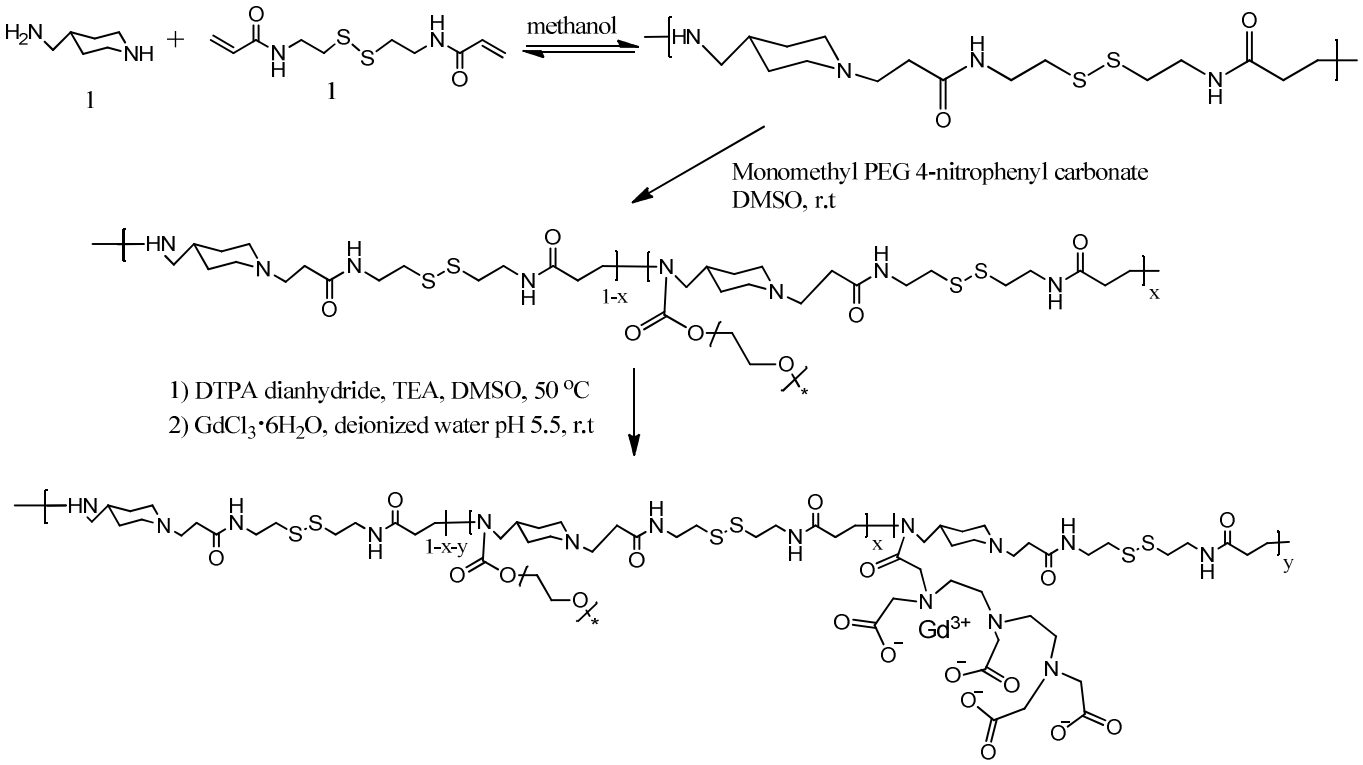

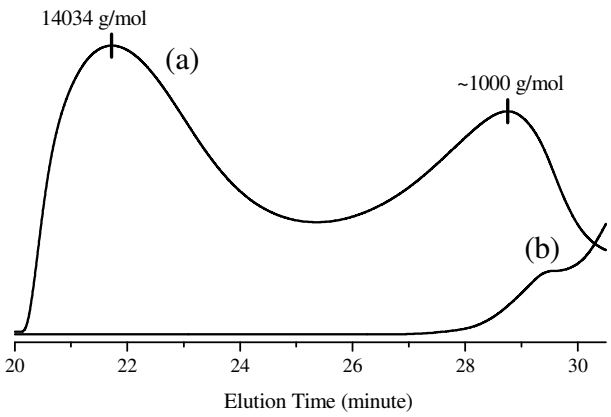

Figure 1. GPC profiles of poly(BAC-AMPD) a) without DTT incubation; b) incubated with 10 mM of DTT at 37°C under stirring for 2 h.

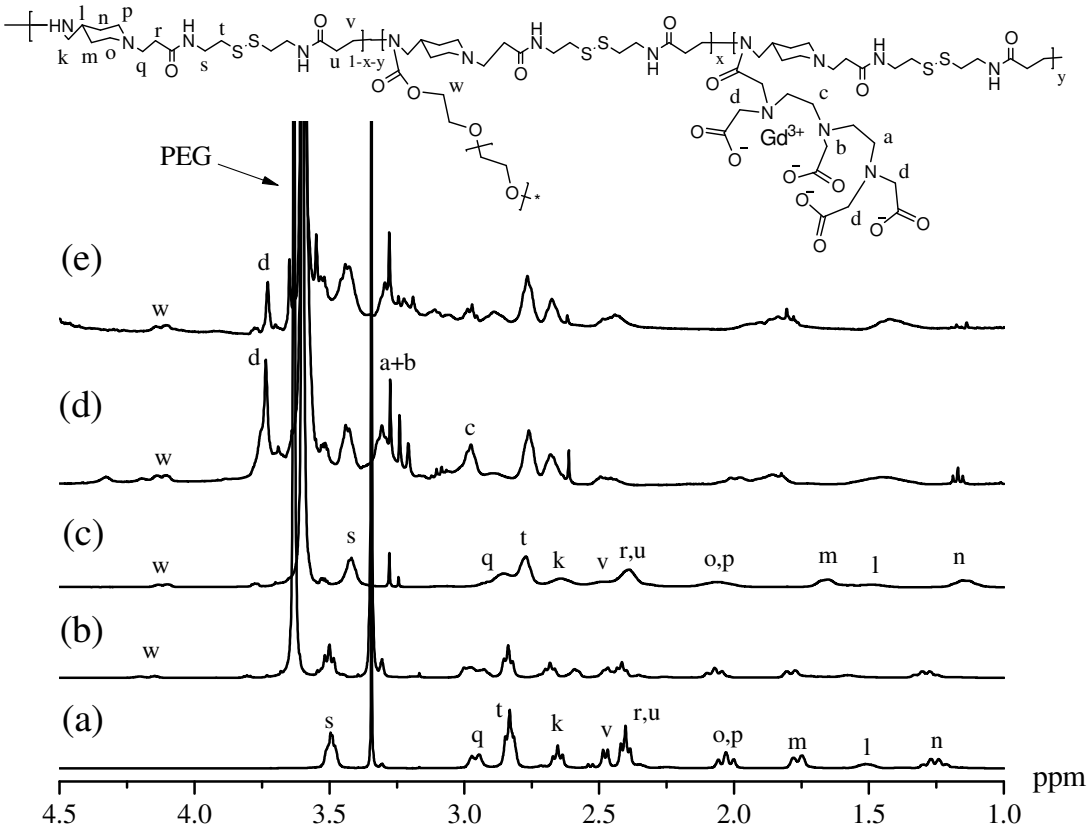

Figure 2. ^{1}H NMR spectra of a) poly(BAC-AMPD) in methanol-d_4; b) poly(BAC-AMPD)-*g*-PEG in methanol-d_4; c) poly(BAC-AMPD)-*g*-PEG in D_2O; d) poly(BAC-AMPD)-*g*-PEG-*g*-DTPA in D_2O at pH 5.5; e) poly(BAC-AMPD)-*g*-PEG-*g*-DTPA in D_2O at pH 7.

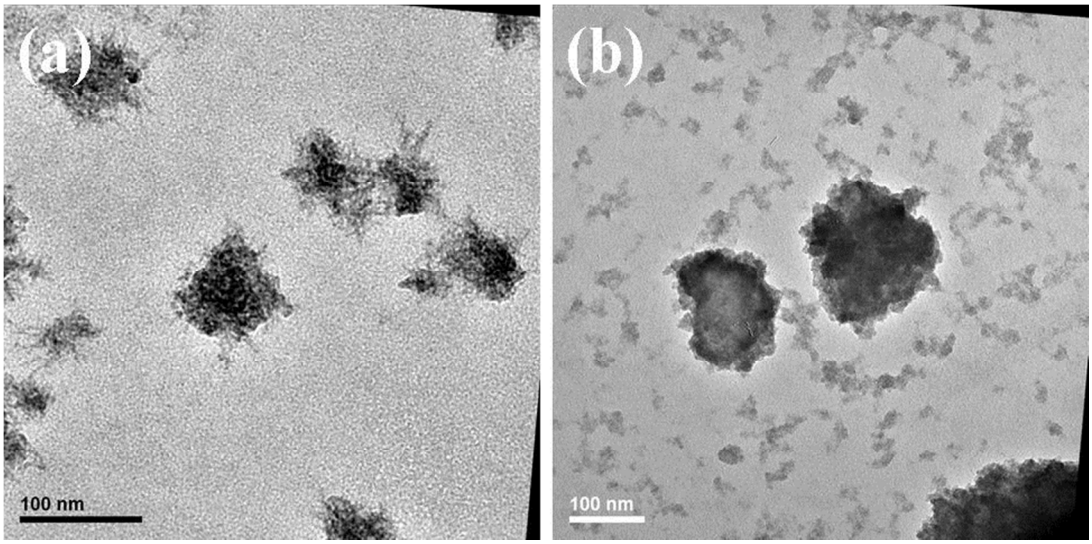

Figure 3. TEM images of the micelles of poly(BAC-AMPD)-*g*-PEG-*g*-Gd-DTPA a) without stain; b) stained with osmium(VIII) oxide.

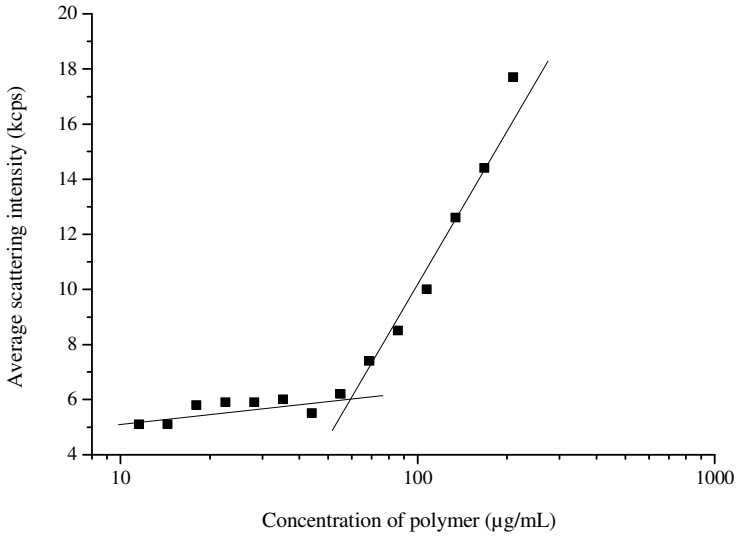

Figure 4. Concentration dependence of the average scattering intensity of DLS from poly(BAC-AMPD)-*g*-PEG-*g*-Gd-DTPA in deionized water.

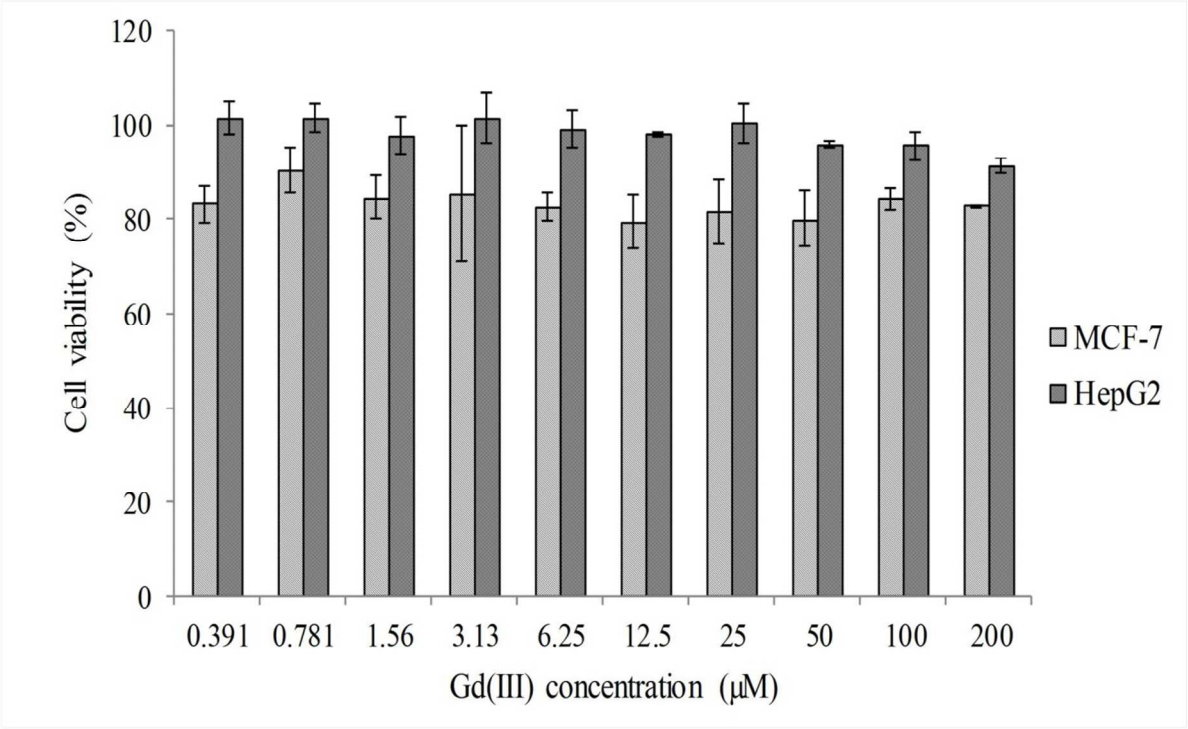

Figure 5. Concentration dependence of *in vitro* cytotoxicity of poly(BAC-AMPD)-*g*-PEG-*g*-Gd-DTPA in MCF-7 and HepG2. All data represent mean ± SD. (n = 3)

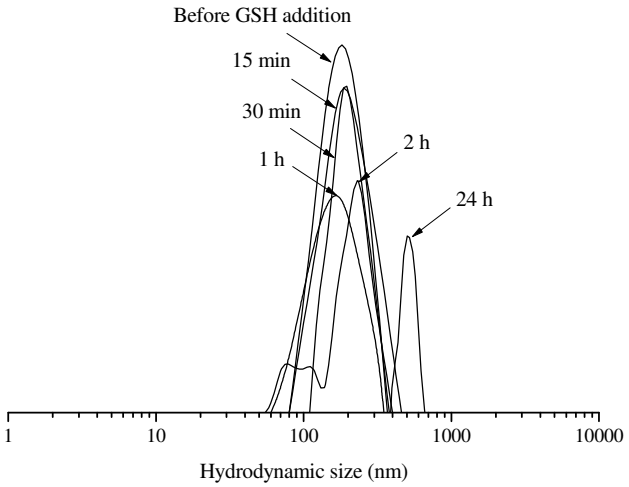

Figure 6. DLS profiles of micelles from 0.5 mg/mL of poly(BAC-AMPD)-*g*-PEG-*g*-Gd-DTPA incubated with 20 μM of GSH at 37 ^{o}C with the intensity being normalized.

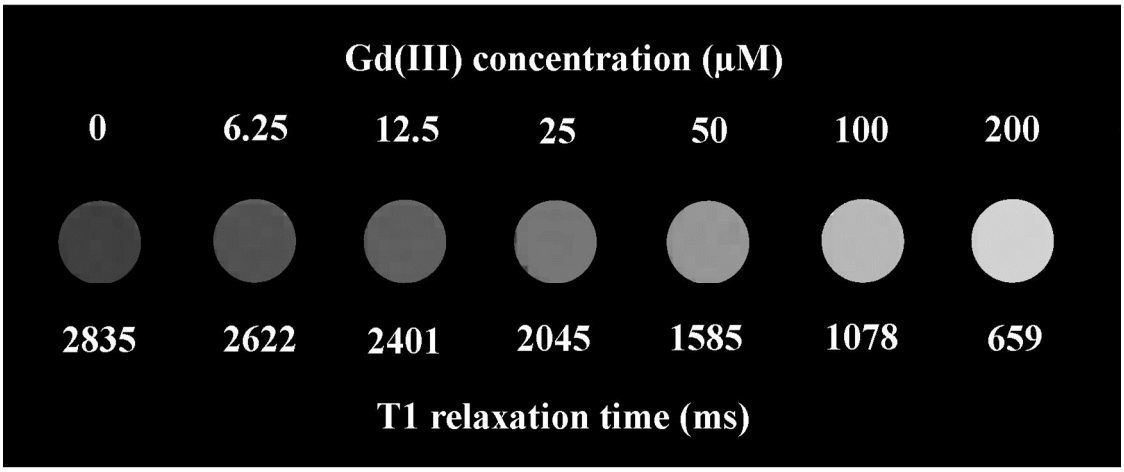

Figure 7. T_1 relaxation time measured at different concentration of Gd(III) of poly(BAC-AMPD)-*g*-PEG-*g*-Gd-DTPA.

Table 1. Dependence of the composition of polymers on the feed

Polymer	Poly(BAC-AMPD)-*g*-PEG	Poly(BAC-AMPD)-*g*-PEG-*g*-DTPA	Poly(BAC-AMPD)-*g*-PEG-*g*-Gd-DTPA
Component	BAC-AMPD / PEG	BAC-AMPD / DTPA dianhydride	BAC-AMPD / $GdCl_3$
Ratio in feed[a]	5 / 1.25	5 / 1 / 20	5 / 1 / 4.2
Ratio in polymer[a]	5 / 1	-	5 / 1.9

[a] in mole

Table of contents graphic

Biodegradable novel polydisulfide MRI contrast agent forming self-assemble in aqueous solution with a low cytotoxicity and a higher r_1 is promising for producing better MRI imaging with lower side effects.